Separation and Purification Technology 118 (2013) 530–539

Contents lists available at ScienceDirect

Separation and Purification Technology

journal homepage: www.elsevier.com/locate/seppur

Coating layer effect on performance of thin film nanofiltration membrane in removal of organic solutes

Emil Dražević [a,*], Krešimir Košutić [a], Vladimir Dananić [b], Dragana Mutavdžić Pavlović [c]

[a] Department of Physical Chemistry, University of Zagreb, Faculty of Chemical Engineering and Technology, Marulićev trg 19, HR-10000 Zagreb, Croatia
[b] Department of Physics, University of Zagreb, Faculty of Chemical Engineering and Technology, Marulićev trg 19, HR-10000 Zagreb, Croatia
[c] Department of Analytical Chemistry, University of Zagreb, Faculty of Chemical Engineering and Technology, Marulićev trg 19, HR-10000 Zagreb, Croatia

ARTICLE INFO

Article history:
Received 15 May 2013
Received in revised form 22 July 2013
Accepted 23 July 2013
Available online 1 August 2013

Keywords:
Nanofiltration
Coating
Membrane modification
Interaction
Organic solutes

ABSTRACT

High affinity of non-ionized hydrophobic organics towards hydrophobic nanofiltration (NF) membranes is often the main cause for their poor removal by NF. Rejection of organics can be increased mostly by making membrane surface hydrophilic and less prone to adsorption. Although numerous studies reported benefits of such surface modifications, very few of them focused on revealing the mechanisms of increased rejection. The present paper aims at comparing measured rejections of various organic solutes of different hydrophilicity/hydrophobicity and sodium chloride on extremely thin NF film membrane, DowFilmTec NF270, before and after coating with poly(vinyl alcohol) (PVA). PVA coating increased the rejection of hydrophobic solutes from 5% to 30%, decreased rejection of hydrophilic solutes from 6% to 50% while the rejections of low interacting solutes, dioxane, and NaCl remained unchanged. Additionally, the rejections of organics of identical molecular mass and similar Stokes radii were compared and found to be governed by the solute/membrane energy of interaction, which correlated with corresponding log K_{ow} values and dipole moments. The removal mechanism of NF270/PVA composite has been proposed based on the difference in measured rejections of solutes and estimated energy of interactions before and after modification.

1. Introduction

High water permeability and rejection of solutes are features which make nanofiltration (NF) membranes economically viable in water softening applications, attractive for water purification and removal of harmful organic solutes from water [1–3]. However, theirs in general hydrophobic selective layer facilitates adsorption and the transport of organic solutes [4–7], which often results with inadequate removal of, for example pesticides, pharmaceuticals and endocrine disrupting compounds, and limits their practical use [5,8,9]. Rejections of non-hydrophobic or ionized organics are generally higher than those of non-ionized hydrophobic solutes due to much lesser solute affinity toward membrane, or charge repulsion through NF membranes. The latter was confirmed in a recent study of Dražević et al. [10] on the RO (SWC1) membrane, where it was shown that non-ionized phenolic solutes enter the selective layer, and freely partition inside by an order of ten, even if solute radius is close to the radius of the pore. Moreover, it was shown that sorption of organics in the selective layer is unfavourable because it changes membrane characteristics in terms of both salts and water permeability.

Nabe et al. [11] correlated membrane surface hydrophilicity with membrane fouling and it can be assumed that rejection of at least some of organics could be improved by rendering the membrane surface more hydrophilic. Furthermore, Norberg et al. [6] found that RO membranes, declared as low fouling, are resistant to fouling in terms of specific flux decrease over time. It is widely accepted today that commercial brackish water RO membranes declared as low fouling, such as BW30 and LFC, have increased oxygen content and are probably coated [12]. Our past study also found [13] that LFC membrane was more resistant to fouling in terms of irreversible pesticide adsorption and flux decrease compared to other membranes.

Many studies focused on surface modification of membranes [14–19] while the general benefits of modifications are permanently reduced membrane fouling [20] and increased rejection of proteins or organic solutes and salts. But, according to authors' knowledge very few were focused on a mechanism which could explain why membranes became better rejecting to some organic solutes while rejections of some solutes remain the same or even decrease. This study aimed at proposing a plausible way to study such mechanism. Commercial thin film NF membrane, NF270, was coated with a thick layer of polyvinyl alcohol (PVA) and the rejections of various organic solutes of different sizes and physicochemical properties were studied before and after the addition of

* Corresponding author. Tel.: +385 14597240.
E-mail address: edraz@fkit.hr (E. Dražević).

1383-5866/$ - see front matter © 2013 Elsevier B.V. All rights reserved.
http://dx.doi.org/10.1016/j.seppur.2013.07.031

PVA layer. Pesticides, bentazone and tebuconazole, were used in this study as model compounds which represent an entire class of high affinity, non-ionized and hydrophobic compounds such as bisphenol A and hormones.

2. Theory

2.1. Concentration polarization corrected rejections

Mass transfer coefficients of solutes used were estimated using a well-known Gröber relation for laminar flow regime [21],

$$Sh = 0.644Re^{0.5}Sc^{0.33}(d_H/L)^{0.33} \quad (1)$$

where Sh is Sherwood number, Re, Reynolds number, Sc, Schimdt number, L, length of the channel and d_H is hydraulic diameter. The number Re is calculated as as $Re = (ud_H)/v$ where u is cross-flow velocity and v is kinematic viscosity. The number Sc is calculated as $Sc = v/D$. Diffusivity of solutes were estimated using Wilke–Chang relation [22]. Hydraulic diameter was estimated using relation proposed by Shock and Miquel [23],

$$d_H = \frac{4(V_{TOT} - V_{SP})}{S_{FC} + S_{SP}} \quad (2)$$

where V_{TOT} is the volume of the channel, V_{SP} the volume of spacer, S_{FC} the surface of the channel and S_{SP} is the surface of the spacer. Mass transfer coefficients were calculated from Sh using the following equation.

$$k = \frac{ShD}{d_H} \quad (3)$$

Measured rejections were corrected for concentration polarization in order to obtain true membrane rejections using well known equation obtained from film theory model [24]. Eq. (4) was used to estimate, f_m, true membrane rejection, which is calculated from measured rejection,f, permeation velocity, J_v, and estimated (Eq. (3)) mass transfer coefficient,k.

$$\frac{1-f}{f} = \frac{1-f_m}{f_m} + \exp\left(\frac{J_v}{k}\right) \quad (4)$$

2.2. Pore size distribution-average pore radii

Pore size distribution (PSD) and average pore radius were calculated using Surface Force-Pore Flow (“SF-PF”) model, which was developed and described by Sourirajan and Matsuura [25]. Briefly, fundamentals of this model are; the pores in the selective layer are assumed to be cylindrical, and solute membrane interactions relative to water can be described as Lennard–Jones surface potential functions. Thorough description of calculation procedure is found in Appendix. Calculation procedure is searching for a pore size distribution which will give minimal deviation between the measured and predicted rejections and permeation velocities of five disk like molecules: 1,3-dioxolane, 1,4-dioxane, 12-crown-4, 15-crown-5 and 18-crown-6. Dominant peak in pore size distribution was taken as the average pore radius which was used in the following section to properly evaluate energy of interactions.

2.3. Energy of interactions

Spiegler–Kedem model modified by Verliefde et al. [4] was used to calculate solute–membrane affinity in terms of energy of interaction:

$$f_m = 1 - \frac{(1-\lambda)^2\exp\left(-\frac{\Delta G}{k_B T}\right)K_C}{1 - \left(1-(1-\lambda)^2\exp\left(-\frac{\Delta G}{k_B T}\right)K_C\right)\exp\left(-\frac{J_v K_C \Delta x}{K_D D \varepsilon}\right)} \quad (5)$$

where f_m is true membrane rejection, $\lambda = r_{St}/r_p$, r_{St} is Stokes radii of a solute and r_p is average pore radius, ΔG is free energy of interaction, T is temperature in K, k_B is Boltzmann constant (J K^{-1}), Δx is thickness of a swelled selective layer, 19 nm for NF270 respectively [26], ε is porosity expressed as water content, 0.2 for NF270 respectively, and J_v is measured permeation velocity (ms^{-1}). Hindrance factors, K_D and K_C, were taken from [4] and are described in following equations:

$$K_D = 1 - 2.3\lambda + 1.154\lambda^2 + 0.224\lambda^3 \quad (6)$$

$$K_C = (2-(1-\lambda)^2)(1 + 0.054\lambda - 0.998\lambda^2 + 0.441\lambda^3) \quad (7)$$

From the experimental data on permeation velocities and rejections, energy of interaction is estimated, as one and only fitting parameter.

3. Experimental methods

3.1. Materials

All of the chemicals used were of analytical grade. Organic solutes used in this study (Table 1) were supplied from different manufacturers: methylisobuthylketone (98%, Riedel-De Haen Ag Seelze, Hannover, Germany); 3,3-dimethyl-2-butanone (98%, Sigma Aldrich, Steinheim, Germany); cyclohexanol (99%, Riedel-De Haen Ag Seelze, Hannover, Germany); oxepane (98%, Heraeus, Karlsruhe, Germany); 4-aminopiperidine (Sigma Aldrich, St. Louis, MO), trimethylene oxide (97%, Across Organics, New Jersey, USA);

Table 1
Physico-chemical properties of selected organic solutes.

Organic solutes	M/g mol^{-1}	log K_{ow}[a]	Dipole moment/Debye[b]	r_{St}/nm[c]
Methyl-isobuthylketone (MIBK)	100.16	1.3	3.9	0.31
3,3-Dimethyl-2-butanone (33D2B)	100.16	1.2	2.9	0.31
Oxepane	100.16	1.9	2	0.29
Cyclohexanol (CHOL)	100.16	1.2	2.4	0.29
4-Aminopiperidine (4AP)	100.16	0.32	3.4	0.28
1,3-Dioxolane	74.08	−0.4	2.3	0.20
1,4-Dioxane	88.11	−0.3	0	0.23
12-Crown-4	176.21	−0.9	2.7	0.35
15-Crown-5	220.27	−1.1	1.6	0.39
18-Crown-6	264.32	−1.4	0.2	0.44
Tebuconazole	307.83	3.7	8.6	0.50
Bentazone	240.28	2.3	3.1	0.38

[a] Partition coefficient of a solute between n-octanol and water, taken as experimental if available in [27].
[b] Dipole moment of a solute calculated by Gaussian software [28].
[c] Calculated from diffusion coefficient of a solute in dilute water solutions estimated by Wilke–Chang equation [29].

1,3-dioxolane (99.8%, Sigma–Aldrich, USA); 1,4-dioxane (99.8%, Sigma–Aldrich, USA); 12-crown-4 (98%, Fluka, Switzerland); 15-crown-5 (98%, Merck-Schuchardt, München, Germany), and 18-crown-6 (99.5%, Fluka, Switzerland). Poly(vinyl alcohol) (PVA) was supplied from Across Organics, and had following molecular masses and hydrolysis degrees: 86,000 (99–100%), 16,000 (98%). Maleic acid (99%, Kemika, Zagreb, Croatia) was used for grafting of the PVA layers. Pesticides used were tebuconazole (99.9%, Bayer, Germany), and bentazone (99.9%, BASF, USA). They were kindly supplied by the Croatian Centre for Agriculture, Food and Rural Affairs, where they are used as analytical standards. The nanofiltration membrane tested and modified was flat sheet type NF270 supplied from Dow/Filmtec, Midland, MI, USA. Prior their use, either for modification or nanofiltration tests, membrane samples were immersed in 1:1 water/ethanol solution for 10 min in ultrasonic bath, and after that immersed into deionized water for 24 h to remove any chemical residues.

3.2. Coating of NF270 with PVA

Membrane samples pre-treated as described in Materials section were coated in several steps as follows:

(1) Wet membrane sample (0.02 m^2) was attached to a glass plate and immersed in a bath of 0.25 mmol dm^{-3} of PVA for 5 min.
(2) Membrane sample on a glass plate was pulled out of the bath and any excess of the PVA solution was removed with a glass roller.
(3) Membrane sample was dried at 60 °C for 1 h.
(4) Membrane sample covered with dry PVA was immersed in a maleic acid solution in ultrasonic bath for 10 min. One liter of solution contained maleic acid (expressed in weight percentages as 0.05%, 0.15%, 0.3%, 0.5% and 1%, respectively), water, 20 ml of concentrated H_2S0_4, and 200 g of Na_2S0_4. Sodium sulfate inhibited the solubility of the PVA dry film in water.
(5) Modified sample was washed with water and treated with 1% aqueous HCl at room temperature for 1 h. After washing with deionised water it was immersed in dilute sodium bicarbonate solution to remove any acid residues. Again washed with DI water, it was stored in DI water before any further tests.

3.3. Fourier transform infrared spectroscopy-attenuated total reflectance (FTIR-ATR) measurements of membrane samples

Membrane samples were characterized by means of FTIR spectroscopy using a Bruker Vertex 70 equipped with a Platinum ATR single reflection diamond ($n = 2.4$) crystal-based module in the mid IR range (400–4000 cm^{-1}). Infrared (IR) spectra of membranes were recorded at 4 cm^{-1} resolution and 24 scans before and after tests with pesticides. Prior FTIR-ATR measurements samples were dried at 50 °C for 24 h in order to remove any residues of water.

3.4. Contact angle measurements

Contact angle measurements (sessile drop technique) have been done on Data Physics – Contact angle system OCA, Germany. Prior to each contact angle measurement, flat sheet membranes were pre-treated, as described in Materials section, and afterwards dried in a hood for 1 week. Each measurement lasted for 2 min and curves represented are the average of three independent measurements.

3.5. NF tests

NF apparatus is in detail described elsewhere [10]. Briefly, tests were made in Sterlitech SEPA II cell of a membrane area 0.0138 m^2, and channel dimensions $14.5 \times 9.5 \times 0.17$ cm^3 (length × width × height). The feed from a 5 L tank was circulated through the cell at fluid velocity of 0.27 m s^{-1}. Temperature was held constant at 25.0 ± 0.1 °C. If not noted differently, the pH during tests with organics was held at 7 and at J_v of about 30 μm s^{-1} (about 1.1 MPa). If the pressure was varied, toobtain the rejection vs. permeation velocity dependence of specific solute, it did not exceed over 2 MPa. The recovery rate was very low, up to about 5%.

In tests with small organic solutes (first five in Table 1), feed solution's pH was adjusted to three values, 4, 7 and 9 by adding drops of 0.5 M NaOH or H_2SO_4 solution, so that the conductivity of the feed solution did not increase over 5%, and its contribution to the overall concentration polarization is considered negligible. Concentration of the solutes in the feed varied as follow: organic solutes, 100 mg L^{-1}; pesticides, 20 mg L^{-1}; NaCl, 500 mg L^{-1}.

Concentrations of organics in both retentate and permeate were determined by Shimadzu TOC V_{WS} Total Carbon Analyzer. Concentrations of pesticides were determined by HPLC coupled with diode array detector. After tests with pesticides membrane samples were cut into pieces and stirred in 100 mL of acetonitrile for 24 h at room temperature, in order to determine the amount of pesticides adsorbed in/on the membrane during nanofiltration.

3.6. HPLC setup

Bentazone and tebuconazole were analyzed using Varian ProStar 500 (Walnut Creek, California, USA) high performance liquid chromatography (HPLC) system with ProStar auto sampler, ProStar 230 tertiary pump system, ProStar 330 diode array detector, and thermostated column compartment. The column temperature was maintained at 25 °C and the injection volume was 20 μL. Column, Synergy Fusion-RP 150 mm × 4.6 mm with particle size of 4 μm, (Phenomenex, USA) was used. The mobile phase used was a binary mixture of 0.1% formic acid in water (A) and 0.1% formic acid in acetonitrile (B). A simultaneous mobile phase gradient program was used as described; the elution started with 6 min linear gradient from 60% A to 30% A, then 0.06 min linear gradient back to 60% of A which was maintained to the end of analysis (8 min was a total time of analysis). The flow rate was constant at 2 mL min^{-1}. Corresponding peaks of tebuconazole and bentazone, which were used for calibration curves and quantification, were found at absorbance wavelengths of 200 nm and 220 nm, respectively. Limit of detection (LOD) of above described method was 1 ppm for both tebuconazole and bentazone.

4. Results and discussion

4.1. Characterization of PVA coatings by the means of FTIR spectroscopy and contact angles

Fig. 1A compares IR spectra of virgin NF270 and PVA coated NF270 membrane. IR spectra (Fig. 1A) of virgin NF270 membrane is identical to one recorded by Tang et al. [12]. PVA can be associated with two major peaks (Fig. 1A and B), C—H broad alkyl stretching band (ν = 2850–3000 cm^{-1}) and hydrogen bonded OH band (ν = 3200–3570 cm^{-1}) [30]. Grafted PVA coatings membrane samples reveal two new signals attributed to MA (Fig. 1C); at 1650 cm^{-1} weak alkenyl (C═C) stretch (ν = 1620–1680 cm^{-1}) [31,32]. Inspection of Fig. 1B and C suggests that the decrease in OH band of PVA, or increase in signal attributed to COOH groups, are more or less proportional to the MA concentrations. Signals

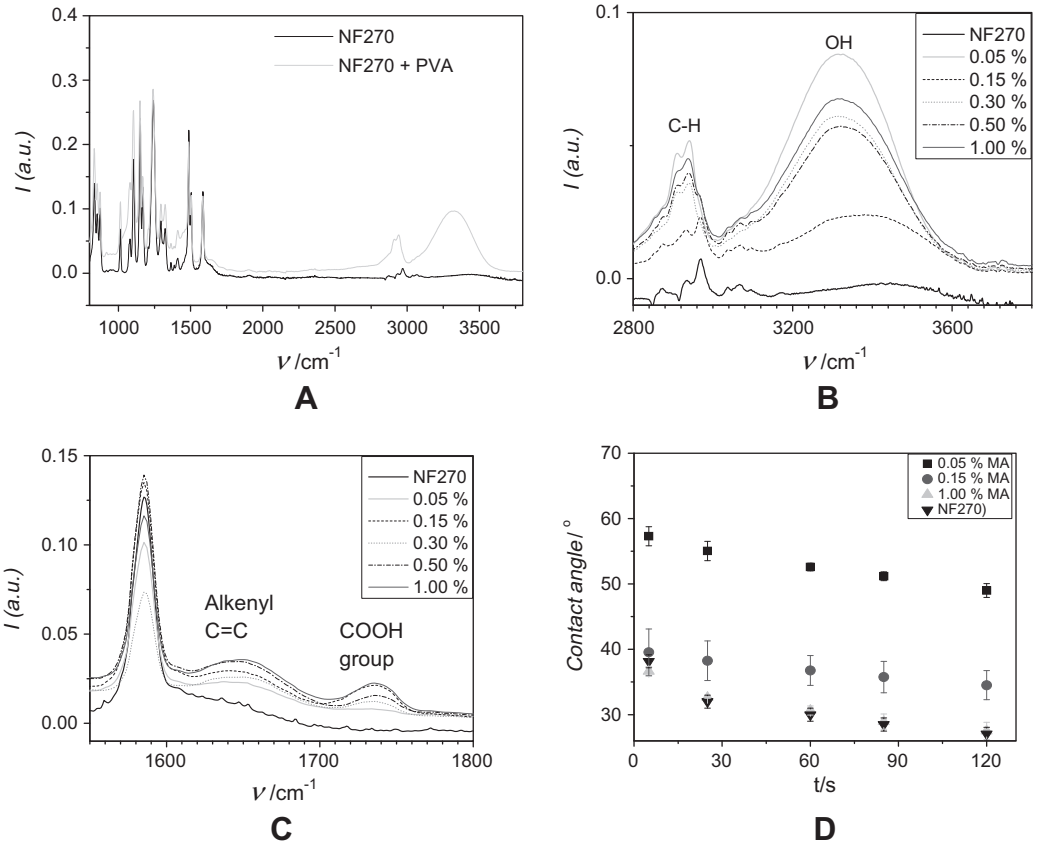

Fig. 1. (A) IR spectra of virgin NF270 and coated PVA NF270 membranes. (B) Decrease in signal strength of OH groups with the increase in concentration of MA. (C) FTIR spectra of coated and grafted NF270 membrane samples. (D) Contact angles of water vs. time on PVA grafted with different concentrations of MA.

are not completely proportional due inability of making PVA films of exactly the same thickness, therefore stoichiometry was not easily controlled. Reaction path is supposed to be esterification of COOH group of MA to OH groups of PVA [33,34].

Contact angles of PVA coated NF270 (Fig. 1D) have higher values compared to virgin NF270. This may be misleading because dry PVA is highly crystalline which ostensibly makes it as hydrophobic surface. On contrary to what Fig. 1D suggests, PVA is extremely hydrophilic as material due high concentration of OH groups, swelling and its high solubility in water [30–34]. Nevertheless, grafting with MA seems to be important because increased concentration of COOH groups seem to improve the overall surface hydrophilicity of the dry PVA coating on top of NF270 (Fig. 1D).

4.2. PVA effect on rejection of low interacting solutes, NaCl and dioxane

Data for all solutes on measured rejection, f, are corrected for concentration polarization (CP) using Eq. (4) to obtain true membrane rejection, f_m. True membrane rejections of NaCl measured at different permeation velocities, i.e., pressures, are summarized in Fig. 2A. Almost no difference in rejections of NaCl measured on PVA coated NF270 and virgin NF270 (Fig. 2A) suggests that PVA does not affect rejection of salts. Curiously, increased content of carboxylic groups (Fig. 1C), i.e., charge on PVA coatings (Fig. 2A) did not contribute to the overall rejection of salts. However, in terms of water permeability PVA coating significantly increased hydraulic resistance because it decreased the L_p (L m^{-2} h^{-1} bar^{-1}) from 12 to about 6 (Fig. 2A).

Dioxane (Fig. 2B) showed similar behavior as NaCl where hydrophilic PVA coating did not affect its rejection as well. Non-ionized dioxane is a neutral molecule with vanishingly small dipole moment and low log K_{ow} (see Table 1), 0 and -0.30, respectively. Organic solutes with small dipole moments and log K_{ow}, analogous to dioxane tested here, are less prone to adsorb on the membrane surface [35] and are better rejected by membranes, which could explain its low interaction with PVA coating as well. Dioxane, similar to NaCl, did not interact with the PVA coating.

4.3. Rejection of hydrophobic organic molecules of similar Stokes radii on pristine NF270-correlation with their physicochemical properties

Pore size distribution of NF270 was calculated following the calculation procedure described in Appendix by using the experimental data on measured rejections and J_v and estimated mass transfer coefficients of five disk like molecules presented in Table 2. NF270 showed bimodal PSD (Fig. 3) where the average pore radius and dominant peak is located at 0.41 nm, with small number of defects (1 defect on 100 of normal pores) at about 0.98 nm. Theoretical rejections and permeation velocities (Table 2) show fairly nice congruence with the corresponding experimental data. A similar average pore radius for NF270 was recently estimated (0.42 nm) by Semião and Schäfer [7] while defects in NF270 (Fig. 3) were reported earlier in TEM surface study of NF270 performed by Pacheco et al. [36].

The scope of this section is to compare rejection of five hydrophobic organic solutes (first five rows in Table 1) on NF270 at different pH (Fig. 4A). The similarity of aforementioned solutes is indicated with their identical molecular mass and similar Stokes radii, where their differences are in dipole moments and log K_{ow} values. Given that the average pore radius (Fig. 3) is constant and Stokes radii of tested five solutes are fairly identical, friction force

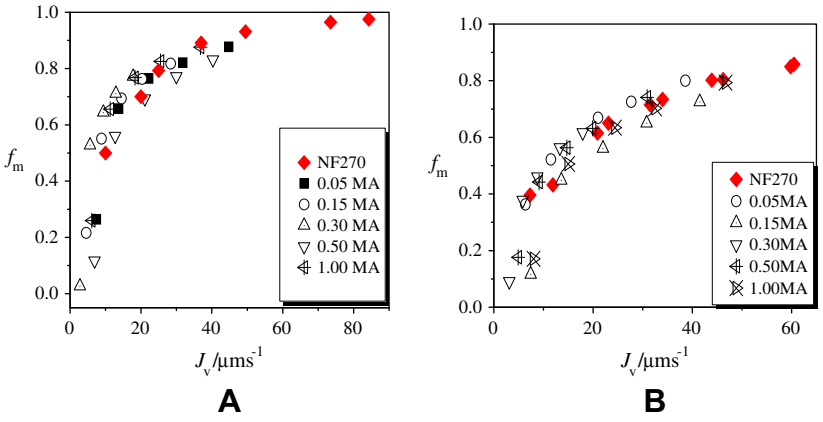

Fig. 2. Comparison on CP corrected rejections between NF270 and PVA coated NF270, pH = 7, t = 25 °C, p = 0.3–2 MPa. (A) f_m (NaCl) vs. J_v. (B) f_m (dioxane) vs. J_v.

Table 2
Comparison of measured and theoretical rejections and permeation velocities, at 1.1 MPa.

Solute	NF270			
	f	f_{theor}	J_v	$J_{v,\ theor}$
1,3-Dioxolane	0.192	0.211	35.6	34.4
1,4-Dioxane	0.435	0.428	32.7	34.4
12-Crown-4	0.944	0.941	33.3	34.4
15-Crown-5	0.945	0.945	34.7	34.5
18-Crown-6	0.955	0.957	34.4	34.5

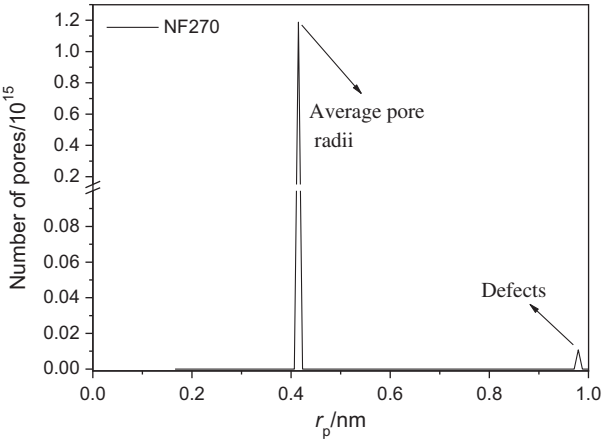

Fig. 3. Pore size distribution of NF270 membrane.

(steric hindrance) could be considered constant. It can be assumed then that physicochemical interactions govern rejection of these solutes by NF270.

Methyl-isobuthylketone (MIBK) and 3,3-dimethyl-2-butanone (33D2B) are isomers with the same number of atoms. These two solutes have (Table 1) fairly similar log K_{ow} values while they differ in MIBK having larger dipole moment. Interestingly, (Fig. 4A) NF270 removed about 63% of MIBK and 80% of 33D2B. Solutes with dipole moments higher than 3 Debye, analogous to MIBK considered here, are less rejected by nanofiltration membranes [37]. Lower rejection could be explained by electrostatic attraction between the opposite pole of dipole and the negatively charged membrane, because molecules in chaotic movements near the membrane wall tend to preferentially orient towards the membrane with the opposite charge of the dipole [37]. However, this explanation would not hold in the present paper given that there is an increase in rejection of solutes (Fig. 4A) with increase in NF270 charge (pH) [6]. Plausible explanation for lower rejection of MIBK, i.e., solutes with higher dipole moment, could be found in preferential physical sorption. Molecules with higher dipole moment form hydrogen bonds with polar groups (—NH_2 or —COOH) in NF270 membrane. Both solutes and water compete for the polar sites in the membrane, and when the solute has significantly higher dipole moment than water it could be preferentially absorbed. Once solutes are preferentially adsorbed to polar sites (COOH, NH_2 groups) in the membrane, they penetrate faster through the membrane nanoporous structure reducing overall membrane rejection.

Similarly, NF270 removed about 66% of CHOL and 74% of oxepane, which differ in both dipole moments and log K_{ow} values (Table 1). However, it should be noted there is no experimental value on log K_{ow} of oxepane found in the literature, and the value calculated by EPISUITE software [27] could deviate from the true experimental value. This assertion could be true since CHOL and oxepane have similar structures, number and type of atoms. It can be assumed then, if logK_{ow} of oxepane and CHOL are similar, that dipole moments govern the rejection of these solutes as well.

Ionized organic solute 4-aminopiperidine (4AP) is a weak base [38], and positively charged in water because both the nitrogen in piperidine ring and primary amine are proton acceptors. It can be noticed in Fig. 3A that its high rejection is going up with the increase of pH, showing similar behavior as other solutes. This is counter-intuitive because NF270 is negatively charged at pH above 4 [39] and one would expect decrease in rejection of 4AP because of electrostatic forces. Perhaps 4AP is well rejected by NF270 because it is completely soluble in water, and its log K_{ow} value is 0.3, making it neutral or low interacting solute. 4AP could be also similar to low interacting dioxane (r_{St} = 0.23 nm, log K_{ow} = −0.3), which measured rejection of f_m = 0.75 at 30 μm s^{-1} is higher than the rejections of MIBK, oxepane and cyclohexanol (CHOL), and very close to the rejection of 33D2B, even though dioxane Stokes radius is much lower than the Stokes radius of the four aforementioned.

As noticed before, all five solutes (Fig. 4A) are better rejected at higher pH. Membrane charge was apparently not the governing factor given that rejection of both non-ionized and ionized solutes (4AP) increased with pH. The reason for this may be fundamental. The slopes ($\Delta J_v/\Delta P$) increased with pH (Fig. 4B), 3.69, 3.77 and 3.82 μm s^{-1} bar^{-1} at pH 4, 7 and 9, respectively. Piperazine amide based membranes (analogous to NF270 tested here) exhibit higher swelling at higher pH [26], i.e., have higher water content, which results with higher water permeability [40] at the same pressure. Higher water content in NF270 membrane made it more permeable to water, while the permeability of solutes remained constant which resulted with more diluted permeate and ostensibly higher

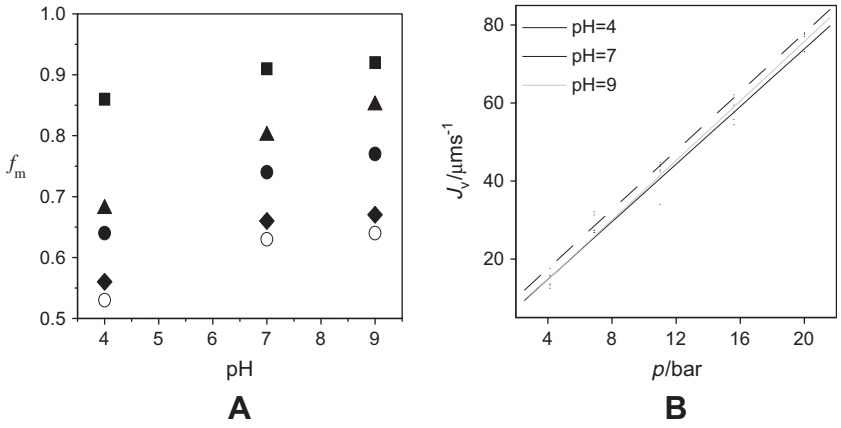

Fig. 4. The average of two independent measurements on NF270 membrane: (A) Rejection as a function of pH at 1.1 MPa, $J_v \approx 30$ μms^{-1} (○ – MIBK, ♦ – CH–OL, ● – oxepane, ▲ – 33D2B, ■ – 4-AP). (B) Linear fits, permeation velocities vs. pressure at different pH.

rejection of solutes. Given that increase in swelling with pH is too small, about 2% [23], to significantly affect membrane properties (porous structure) in terms of permeability to solutes, increased rejection could be explained by increase in J_v (Eq. (5)).

4.4. Energy of interactions of hydrophobic solutes with similar Stokes radii on NF270 and PVA/NF270-correlation to log K_{ow} and dipole moments

True membrane rejections of five hydrophobic solutes of the same radius increased from 6% to 15% after the addition of hydrophilic PVA layer grafted with 1% of MA (Fig. 5). Following discussion is facilitated by comparing the experimental data on NF270 and PVA coated NF270 membranes through energy of interactions (ΔG), calculated using the model described in the theoretical part (Eq. (5)). In both cases, with or without PVA layer, 19 nm [26] was taken as a thickness of the selective layer and 0.2 [26] as water content, because, as shown in previous chapter on examples with salts and dioxane, the rejection of PVA/NF270 composite is determined only by NF270 beneath. Fairly good congruence between the experimental data and the fits in Fig. 5B provides proof on applicability of the same model with one thickness and water content.

It can be noticed (Fig. 5C and D) that MIBK showed negative ΔG value on pristine NF270 which could be interpreted as MIBK freely partition or adsorb in the membrane porous structure [4]. Negative ΔG, which is attributed to very high dipole moment and the high log K_{ow} value of MIBK, is the main cause for its poor rejection by NF270 (Fig. 4A). NF270 in general showed higher affinity for hydrophobic solutes where all solutes except oxepane seem to follow the trend (Fig. 5C) of decreasing ΔG with increasing log K_{ow}. As noted before, oxepane could deviate from the trend in Fig. 5C because there is no experimental value of log K_{ow} or water solubility of this solute found in the literature. Curiously, oxepane, CHOL and 33D2B (Fig. 5C) have fairly similar ΔG on both NF270 and NF270/PVA which could indicate they have similar log K_{ow}.

Still, the trend (Fig. 5C) could be counterintuitive given NF270 membrane is considered hydrophilic [39,41,42] In this context, general trend in Fig. 5C suggests that NF270 membrane is not truly hydrophilic membrane but rather less hydrophobic compared to other membranes [6] probably due increased concentration of COOH groups at its surface.

Interaction energy correlates well with dipole moments of the solutes tested (Fig. 5D) given that only 4AP deviates from the trend. It should be noted that 4AP is completely soluble in water and its log K_{ow} value is very close to zero, compared to the other four (Table 1) which could have similar log K_{ow} values, as discussed earlier. Apparently, the dominant parameter which governs rejection and determines ΔG on the same membrane is hydrophobicity of the solutes (log K_{ow}). Addition of PVA layer on NF270, i.e., change in affinity of membrane, shifted up the values of ΔG and increased rejections, but, interestingly, the general trends (Fig. 5C and D) remained similar, for all five solutes considered.

4.5. Rejections of hydrophilic solutes on NF270 and PVA/NF270 membranes – effect of solute size and log K_{ow}

Data on Stokes radii and log K_{ow} of hydrophilic solutes, 1,3-dioxolane, 12-crown-4, 15-crown-5 and 18-crown-6, are listed in Table 1. It can be noticed in general, that the rejections of hydrophilic solutes on NF270 decreased after addition of PVA layer (Fig. 6A). Fig. 6B compares the difference in measured rejections (%) of hydrophilic solutes as a function of λ. Parameter λ is calculated as the ratio between Stokes radii of the molecules and the average pore radius of NF270 (0.41 nm), thus 1,3-dioxolane, which has λ of only 0.5, could be considered as smallest solute relative to average pore radius. Indeed, 1,3-dioxolane showed the highest difference in rejection (50%) measured on NF270 and NF270/PVA which could be attributed to low friction force experienced with the membrane pore wall and its high interaction with PVA layer. Concentration of 1,3-dioxolane in PVA, could be higher than one in the feed solution, therefore, its big change in rejection could be attributed to the change in its concentration near the membrane surface after the addition of PVA layer.

Fig. 6A shows that rejections of 12-crown-4, 15-crown-5 and18-crown-6, of which λ are 0.85, 0.95 and slightly above 1, respectively, are close to 97% (Fig. 6A). They were not 100% rejected by pristine NF270 only due existence of small number of defects at 0.98 nm in NF270 selective layer (Fig. 3). It may be noted however, that their rejection decreased with the addition of PVA layer and the trend (Fig. 6A and B, lower scale) of decreasing rejection with the sizes of ethers is conversely of what should be expected. Nevertheless, negative log K_{ow} values (−0.9, −1.1 and −1.4) seem to explain the trend (Fig. 6) fairly well because the biggest 18-crown-6 is also the most hydrophilic, and could have the highest interaction with PVA (Fig. 6B). This explanation may realistically hold for membranes having NF270 properties, such as thin selective layer and small number of defects, which could facilitate the transport of solutes and may add to membrane's sensitivity to changes in concentration, even of larger solutes as will be shown in the following chapter.

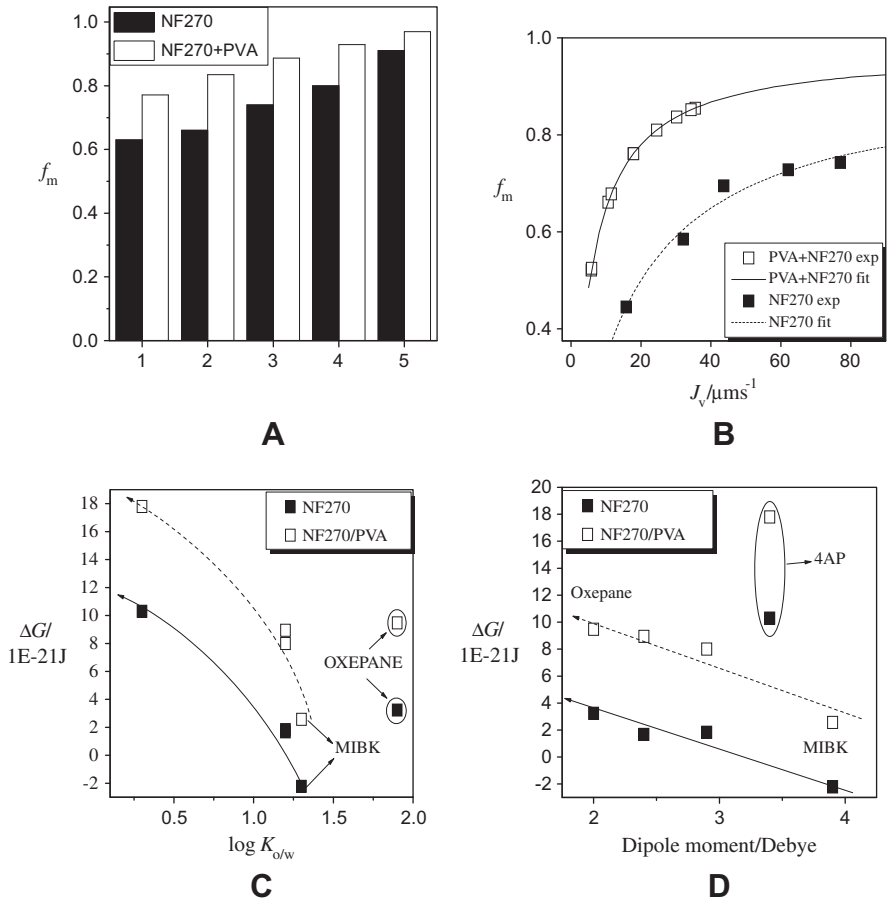

Fig. 5. Comparison of pristine NF20 and PVA (1% MA) coated NF270 as an average of two independent measurements on five solutes: (A) Rejections of five solutes at pH = 7 and $J_v \approx 30$ μm s^{-1}, (1) MIBK, (2) CHOL, (3) Oxepane, (4) 33D2B, (5) 4AP. (B) Comparison of fit and experimental data, for MIBK. (C) ΔG vs. log K_{ow} value. (D) ΔG vs. dipole moment.

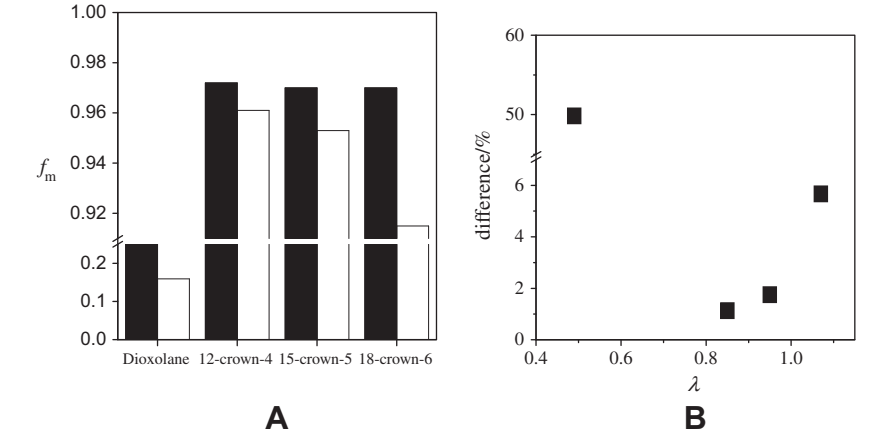

Fig. 6. Rejections of hydrophilic solutes as an average of two independent measurements, bare NF270 (black) and PVA (1% MA) coated NF270 membranes (white): (A) pH = 7 and $J_v \approx 20$ μm s^{-1}; 1,3-dioxolane, 12-crown-4, 15-crown-5 and 18-crown-6. (B) The differences between measured rejections (%) on NF270 and PVA/NF270 membranes as a function λ.

4.6. Adsorption and removal of pesticides – comparison of NF270 and PVA coated NF270 membranes

Concentrations of model hydrophobic compounds, pesticides (Table 1) bentazone and tebuconazole, were unusually high in this study, 20 mg L^{-1}, compared to one thousand times smaller concentrations usually found in wastewaters. It may be noted that the rejection of hydrophobic solute is accurately measured after membrane is saturated with the examined solute [43], and the usage of high concentrations may facilitate saturation. In addition, Chang et al. [44] have reported 100% rejection of estrone at small concentrations with hollow fiber microfiltration membrane, where the

mechanism of removal could be adsorption because the pores were large and rejection of estrone has decreased with time when membrane was saturated.

In this study, tebuconazole has been detected in the extract of NF membrane samples after tests. Tebuconazole was found in large quantity as presented in Fig. 7A, while bentazone remained undetected. High permeate concentration (2.5 ppm) of tebuconazole suggests that solutes which show high affinity for the membrane significantly pass through defects in NF270, similarly as noted earlier for 18-crown-6 on NF270/PVA. Addition of PVA layer reduced the adsorption of tebuconazole for about 3.6 times, while the concentration of tebuconazole in permeate was reduced from 2.5 to 0.5 mg L^{-1}, giving rejections above 95%. Fig. 7A is direct evidence on rejection mechanism of NF270/PVA because reduced adsorption (concentration of the tebuconazole) at the PVA/NF270 surface correlates well with reduced permeate concentration and thus rejection. The amount of tebuconazole adsorbed was huge and best case, using NF270 coated with PVA and grafted with 1% of MA, it adsorbed about 1.4 mg (membrane surface 138 cm^2). High adsorption of tebuconazole could have been caused by reaching the solubility limit during nanofiltration. However, it could be also reconfirmed [43] that the usage of small concentrations of pesticides (μg L^{-1}) would lead to almost 100% rejections because adsorption capacity of NF270 is obviously big, even though NF270 is considered as hydrophilic membrane. It could take several days of continuous and fresh feed of μg L^{-1} concentrations until the membrane is saturated and show its true rejection.

Fig. 7B and E show two general trends in change of permeate concentrations of pesticides (solutes with strong affinity) on bare

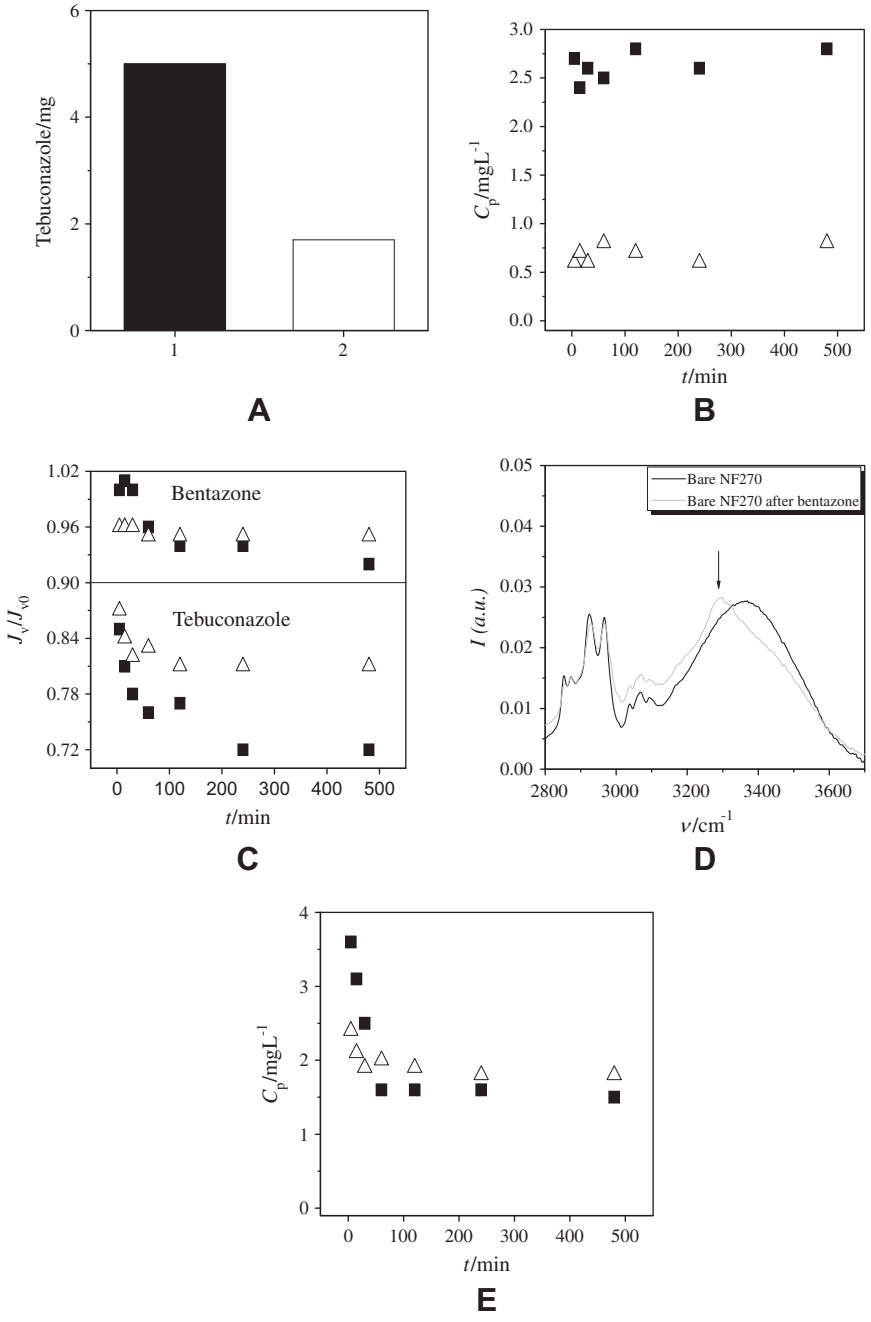

Fig. 7. (A) Adsorbed mass of tebuconazole on NF270 (black) and NF270/PVA (1% MA) (white) membranes. (B) Permeate concentration of tebuconazole vs. time. (C) Flux reduction on membranes. (D) FTIR spectra before and after bentazone (E) Permeate concentration of bentazone vs. time.

NF270 with time. Tebuconazole, which Stokes radius of 0.5 nm is above the average pore radii, 0.41 nm, has shown a constant permeate concentration, even though it adsorbed in large quantity. Adsorption of the tebuconazole considerably reduced the water permeability of bare NF270, for about 30% (Fig. 7C). Bentazone, conversely to tebuconazole, has shown a significant change in permeate concentration with time, where at the beginning of tests its concentration in permeate was high and after 8 h it reduced about 2.3 times, thus increasing NF270 rejection and reducing the overall J_v (Fig. 7C). Bentazone has a Stokes radius (0.38 nm) lower than the average pore radius of NF270, thereby it clogged the pores [35] of NF270 during nanofiltration thus reducing NF270 water permeability and increasing rejection (Fig. 7E). In addition, feed concentration of bentazone changed from 19.7 to 18.7 ppm. Since the volume of the recirculating feed solution was 4 L it means that about 4 mg of bentazone has been lost. All of the piping and feed tank in the system were made of stainless steel, Teflon and glass, therefore all of the bentazone adsorbed could be attributed to NF270 and plastic feed spacer. Indeed, (Fig. 7D) FTIR spectra of bare NF270 after tests with bentazone showed a new peak attributed to N—H stretching of bentazone [45].

It may be noticed that final rejection of bentazone measured at bare NF270 (Fig. 7E) was higher compared to PVA coated NF270. PVA coating reduced clogging thus affecting final permeate concentration (Fig. 7E). Nevertheless, if data are compared at times below one hour, when the clogging is not significant, it can be noticed that PVA significantly affected the rejection of bentazone, similarly as it did for tebuconazole.

5. Conclusions

This study is among very few which examined rejection of hydrophobic organic solutes of identical molecular mass and similar Stokes radii on the same membrane. Similar sizes of these solutes, i.e., almost constant membrane/solute friction forces allowed to evaluate the pure effect of physicochemical properties of solutes on their rejections by membrane. Estimated solute/membrane energy of interactions, of both pristine NF270 and PVA coated NF270, correlated well with experimental log K_{ow}. Similarly, energy of interactions correlated with corresponding dipole moments when experimental log K_{ow} values were of similar values. Addition of PVA layer changed energy of interactions of these solutes towards higher repulsion, however, the trends between energy of interactions, dipole moments and experimental log K_{ow} values remained similar for both NF270 and NF270/PVA.

PVA coating did not affect rejection of NaCl and low interacting solute, 1,4-dioxane, suggesting that it contributes only to rejection of organic solutes which do have affinity to PVA. NF270 membrane, which is considered as hydrophilic membrane, showed a huge adsorption capacity for the pesticides tested and higher affinity for hydrophobic solutes which resulted with their lower removal. Hydrophilic PVA coating considerably improved removal of hydrophobic solutes and reduced the mass of adsorbed hydrophobic pesticide (tebuconazole) thus reducing its final measured permeate concentration.

Given that NF270 membrane has very thin rejecting layer, 19 nm, and looser structure with a small number of defects, it is reasonable to assume that the rejection of solutes by this membrane is highly sensitive to changes in concentration at the feed side of the membrane surface. In this context, PVA did not act as a selective layer but it did contribute to the rejection by affecting the solute/membrane interaction and the concentrations of organic solutes near the membrane wall, thus increasing or reducing the driving force of Fickian diffusion of solutes.

Acknowledgements

The authors are grateful to Mrs. Sandra Milin who did a major part of experimental work in this study. This work was supported by the Croatian Ministry of Science, Education and Sports through Project 125-1253008-3009 "*Membrane and adsorption processes for removal of organic compounds in water treatment*".

Appendix A. Supplementary material

Supplementary data associated with this article can be found, in the online version, at http://dx.doi.org/10.1016/j.seppur.2013.07.031.

References

[1] L.D. Ngheim, A.I. Schaffer, M. Elimelech, Removal of natural hormones by nanofiltration membranes: measurement, modeling and mechanisms, Environ. Sci. Technol. 38 (2004) 1888–1996.
[2] V. Yangali-Quintanilla, S.K. Maenga, T. Fujioka, M. Kennedy, G. Amy, Proposing nanofiltration as acceptable barrier for organic contaminants in water reuse, J. Membrane Sci. 362 (2010) 334–345.
[3] B. Cyna, G. Chagneau, G. Bablon, N. Tanghe, Two years of nanofiltration at the Méry-sur-Oise plant, France, Desalination 147 (2002) 69.
[4] A.R.D. Verliefde, E.R. Cornelissen, S.G.J. Heiman, E.M.V. Hoek, G.L. Amy, B.V.D. Bruggen, J.C.V. Dijk, Influence of solute-membrane affinity on rejection of uncharged organic solutes by nanofiltration membranes, Environ. Sci. Tech. 43 (2009) 2400–2406.
[5] A.M. Comerton, R.C. Andrews, D.M. Bagley, C. Hao, The rejection of endocrine disrupting and pharmaceutically active compounds by NF and RO membranes as a function of compound and water matrix properties, J. Membrane Sci. 313 (2008) 323–335.
[6] D. Norberg, S. Hong, J. Taylor, Y. Zhao, Surface characterization and performance evaluation of commercial fouling resistant low-pressure RO membranes, Desalination 202 (2007) 45–52.
[7] A.J.C. Semião, A.I. Schäfer, Removal of adsorbing estrogenic micropollutants by nanofiltration membranes. Part A—Experimental evidence, J. Membrane Sci. 431 (2013) 244–256.
[8] A.R.D. Verliefde, E.R. Cornelissen, S.G.J. Heiman, E.M.V. Hoek, G.L. Amy, B.V.D. Bruggen, J.C.V. Dijk, Influence of solute-membrane affinity on rejection of uncharged organic solutes by nanofiltration membranes, Environ. Sci. Technol. 43 (2009) 2400–2406.
[9] A.J.C. Semião, M. Foucher, A.I. Schäfer, Removal of adsorbing estrogenic micropollutants by nanofiltration membranes: Part B—Model development, J. Membrane Sci. 431 (2013) 257–266.
[10] E. Dražević, S. Bason, K. Košutić, V. Freger, Enhanced partitioning and transport of phenolic micropollutants within polyamide composite membranes, Environ. Sci. Technol. 46 (2012) 3377–3383.
[11] A. Nabe, E. Staude, G. Belfort, Surface modification of polysulfone ultrafiltration membranes and fouling by BSA solutions, J. Membrane Sci. 133 (1997) 57–72.
[12] C.Y. Tang, Y.-N. Kwon, J.O. Leckie, Effect of membrane chemistry and coating layer on physiochemical properties of thin film composite polyamide RO and NF membranes I. FTIR and XPS characterization of polyamide and coating layer chemistry, Desalination 242 (2009) 149–167.
[13] E. Dražević, K. Košutić, S. Fingler, V. Drevenkar, Removal of pesticides from the water and their adsorption on the reverse osmosis membranes of defined porous structure, Deswater 30 (2011) 161–170.
[14] A. Ben-David, R. Bernstein, Y. Oren, S. Belfer, C. Dosoretz, V. Freger, Facile surface modification of nanofiltration membranes to target the removal of endocrine-disrupting compounds, J. Membrane Sci. 357 (2010) 152–159.
[15] R. Bernstein, S. Belfer, V. Freger, Surface modification of dense membranes using radical graft polymerization enhanced by monomer filtration, Langmuir 26 (2010) 12358–12365.
[16] R. Bernstein, S. Belfer, V. Freger, Toward improved boron removal in RO by membrane modification: feasibility and challenges, Environ. Sci. Technol. 45 (2011) 3613–3620.
[17] J.-H. Kim, P.-K. Park, C.-H. Lee, H.-H. Kwon, Surface modification of nanofiltration membranes to improve the removal of organic micropollutants (EDCs and PhACs) in drinking water treatment: graft polymerization and cross-linking followed by functional group substitution, J. Membrane Sci. 321 (2008) 190–198.
[18] D. Rana, T. Matsuura, Surface modifications for antifouling membranes, Chem. Rev. 110 (2010) 2448–2471.
[19] Y. Zhang, H. Li, H. Li, R. Li, C. Xiao, Preparation and characterization of modified polyvinyl alcohol ultrafiltration membranes, Desalination 192 (2006) 214–223.
[20] A. Ben-David, S. Bason, J. Jopp, Y. Oren, V. Freger, Partitioning of organic solutes between water and polyamide layer of RO and NF membranes: correlation to rejection, J. Membrane Sci. 281 (2006) 480–490.

[21] V. Gekas, B. Hallström, Mass transfer in the membrane concentration polarization layer under turbulent cross flow I. Critical literature review and adaptation of existing Sherwood correlations to membrane operations, J. Membrane Sci. 30 (1987) 153.
[22] C.R. Wilke, P. Chang, Correlation of diffusion coefficients in dilute solutions, AIChE J. 1 (1955) 264–270.
[23] G. Shock, A. Miquel, Mass transfer and pressure loss in spiral wound modules, Desalination 64 (1987) 339.
[24] S. Sourirajan, T. Matsuura, Chapter 2, in: Reverse Osmosis/Ultrafiltration Process Principles, National Research Council Canada, Canada, 1987, pp. 79–194.
[25] S. Sourirajan, T. Matsuura, Chapter 4, in: Reverse Osmosis/Ultrafiltration Process Principles, National Research Council Canada, Canada, 1987, pp. 279–358.
[26] V. Freger, Swelling and morphology of the skin layer of polyamide composite membranes: an atomic force microscopy study, Environ. Sci. Technol. 38 (2004) 3168–3175.
[27] U.S.E.P. Agency, US EPA. Estimation Programs Interface Suite™ for Microsoft® Windows, v 4.10, in, United States Environmental Protection Agency, Washington, DC, USA, 2011.
[28] M.J.F. et al., Gaussian 09, Revision A.02, in, Gaussian, Inc., Wallingford, CT, USA, 2009.
[29] B.E. Poling, J.M. Prausnitz, J.P. O'Connel, The Properties of Gases and Fluids, McGraw-Hill, New York City, USA, 2001.
[30] E.F.d. Reis, F.S. Campos, A.P. Lage, R.C. Leite, L.G. Heneine, W.L. Vasconcelos, Z.I.P. Lobato, H.S. Mansur, Synthesis and characterization of poly (vinyl alcohol) hydrogels and hybrids for rMPB70 protein adsorption, Mater. Res. 9 (2006) 185–191.
[31] W.-Y. Chiang, C.-M. Hu, Studies of reactions with polymers. I. The reaction of maleic anhydride with PVA and the properties of the resultant, J. Appl. Polym. Sci. 30 (1985) 3895–3910.
[32] R.Y.M. Huang, J.W. Rhim, Modification of poly(viny1 alcohol) using maleic acid and its application to the separation of acetic acid-water mixtures by the pervaporation tech n i q u e, Polym. Int. 30 (1993) 129–135.
[33] C. Zaccone, T.M. Miano, W. Shotyk, Qualitative comparison between raw peat and related humic acids in an ombrotrophic bog profile, Org. Geochem. 38 (2007) 151–160.
[34] A.K. Mishra, D.K. Chattopadhyay, B. Sreedhar, K.V.S.N. Raju, FT-IR and XPS studies of polyurethane-urea-imide coatings, Prog. Org. Coat. 55 (2006) 231–243.
[35] B. Van der Bruggen, L. Braeken, C. Vandecasteele, Evaluation of parameters describing flux decline in nanofiltration of aqueous solutions containing organic compounds, Desalination 147 (2002) 281–288.
[36] C.A. Pacheco, I. Pinnau, M. Reinhard, J.O. Leckie, Characterization of isolated polyamide thin films of RO and NF membranes using novel TEM techniques, J. Membrane Sci. 358 (2010) 51.
[37] B.V.d. Bruggen, J. Schaep, D. Wilms, C. Vandecasteele, Influence of molecular size, polarity and charge on the retention of organic molecules by nanofiltration, J. Membrane Sci. 156 (1999) 29–41.
[38] D.D. Perrin, B. Dempsey, E.P. Serjeant, PKa Prediction for Organic Acids and Bases, Chapman and Hall, New York, 1981.
[39] M. Mänttäri, T. Pekuri, M. Nyström, NF270, a new membrane having promising characteristics and being suitable for treatment of dilute effluents from the paper industry, J. Membrane Sci. 242 (2004) 107–116.
[40] P. Meares, F.H. Stillinger, F. Franks, D.A.T. Dick, The mechanism of water transport in membranes, Philos. Trans. R Soc. Lond. B 278 (1977) 113–150.
[41] M. Mänttäri, A. Pihlajamäki, M. Nyström, Effect of pH on hydrophilicity and charge and their effect on the filtration efficiency of NF membranes at different pH, J. Membrane Sci. 1–2 (2006) 311–320.
[42] K. Boussu, C. Kindts, C. Vandecasteele, B.V.d. Bruggen, Surfactant fouling of nanofiltration membranes: measurements and mechanisms, Chem. Phys. Chem. 8 (2007) 1836–1845.
[43] K. Kimura, G. Amy, J. Drewes, Y. Watanabe, Adsorption of hydrophobic compounds onto NF/RO membranes: an artifact leading to overestimation of rejection, J. Membrane Sci. 221 (2003) 89–101.
[44] S. Chang, T.D. Waite, A.I. Schäfer, A.G. Fane, Adsorption of trace steroidestrogens to hydrophobic hollow fibre membranes, Desalination 146 (2002) 381–387.
[45] D.J. Skrovanek, S.E. Howe, P.C. Painter, M.M. Coleman, Hydrogen bonding in polymers: infrared temperature studies of an amorphous polyamide, Macromolecules 18 (1985) 1676–1683.